ARTICLE

First-Principles Study on Adsorption of Magnesium Porphyrin on Sodium Chloride Covered Au(111) Surfaces

Wenjing Zhao, Jiyin Xiao, Liang Ma, Guangjun Tian*

State Key Laboratory of Metastable Materials Science & Technology and Key Laboratory for Microstructural Material Physics of Hebei Province, School of Science, Yanshan University, Qinhuangdao 066004, China

(Dated: Received on February 23, 2025; Accepted on March 18, 2025)

The adsorption properties of a magnesium porphyrin (MgP) molecule on Au(111) surface covered with up to three layers of sodium chloride (NaCl) were investigated by means of first-principles calculations. The most stable adsorption configuration of MgP on the NaCl/Au(111) heterosurfaces was found to be at the Cl-top site with a 20° angle between the [1$\bar{1}$0] lattice direction of NaCl and the Mg–N bond of the molecule. Compared with MgP molecule adsorbed on bare Au(111), the inclusion of NaCl layers can lead to a significant decrease in the adsorption energy of the MgP molecule. The existence of NaCl layers also reduced the charge transfer between the molecule and the surface. For heterosurfaces with two or three monolayers of NaCl, the charge transfer was almost completely suppressed. The obtained partial density of states (PDOS) showed that hybridization between the electronic structures of the adsorbed MgP molecule and the metal surface can be significantly suppressed when NaCl layers were added. For the heterosurface with three layers of NaCl, the PDOS around the Fermi level was almost identical with that of the free molecule, suggesting the electronic structure of the MgP molecule was nicely preserved. Influence of the NaCl layers on the electronic structure of the MgP molecule was mainly found for molecular orbitals (MOs) away from the Fermi level as a result of the large band gap of the NaCl layers.

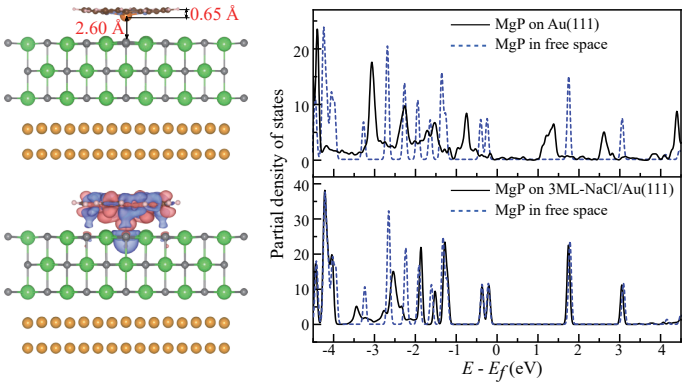

Key words: Surface adsorption, First-principles calculation, Porphyrin, Sodium chloride

I. INTRODUCTION

A detailed understanding of the adsorption properties of molecular systems on solid surfaces is vital in many fields such as heterogeneous catalysis [1], gas sensing [2], and molecular electronics [3]. As one of the most important surface characterization tools, scanning tunneling microscope (STM) is invaluable for the study of the adsorption of molecular systems on metallic surfaces. STM also has the ability to investigate the electronic structures such as the spatial distributions of the frontier molecular orbitals (MOs) of adsorbed molecules [4, 5]. An important condition for the success of such advanced characterization is to minimize the direct metal–molecule interaction that can strongly affect the electronic structure of the sample. Such a re-

* Author to whom correspondence should be addressed.
E-mail: tian@ysu.edu.cn

quirement can be achieved by adding thin decoupling layers to the metal substrates [4]. The decoupling layer should be easy to grow on metal surfaces with appropriate thickness and have a sufficient band gap to reduce the electronic interaction between the sample and the substrate [4, 6, 7].

Many types of materials, such as metal oxides [8–11], two dimensional (2D) materials [12–16], and alkali halide (NaCl) [4, 17, 18] have been successfully applied to decouple single-molecules from the metal substrate of STM. Among those materials, NaCl, which has a wide band gap [4], is one of the most commonly used decoupling materials because defect-free multi NaCl layers can be conveniently fabricated on different metal surfaces [4, 5, 18–20]. It is also one of the first decoupling materials that was applied to decouple adsorbed molecules and obtain STM images of individual MOs [4]. Since then, thin NaCl layers have found application in many STM based single-molecule measurements, such as STM-induced electroluminescence [17, 18, 21–25] and STM tip-enhanced photoluminescence [26, 27].

Since the growth of NaCl on metal surfaces is well defined, NaCl layers from monolayer to multi-layer can be readily obtained experimentally. Recent experiments have shown that the molecular response, such as the charge-state lifetimes [28] and electroluminescence spectra [22] of single-molecules, could vary as the thickness of NaCl changes. This suggests that the number of NaCl layers between the metal substrate and the molecule could affect the adsorption properties of the molecule. To this end, it is worthwhile to investigate the influence of different layers of NaCl on the adsorption of molecular systems on metal surfaces. In a previous work, we have studied the adsorption properties of a double-decker paracyclophane molecule on NaCl/Au(111) surfaces [29] with the aim of proving the feasibility to construct a special type of charge-transfer based single-molecule switches [30]. Compared with the paracyclophane molecule, metalloporphyrins are more commonly used in STM measurements due to their novel geometrical and electronic properties [31–33]. Thus, it is desirable to investigate the adsorption of such systems on metal/decoupling-layer heterosurfaces such as NaCl/Au.

In a recent work, we have studied the adsorption properties of magnesium porphyrin (MgP), which is a commonly used metalloporphyrin in STM measurements [34,35], on graphene and hexagonal boron nitride monolayer covered Au(111) surfaces [36]. The present work is devoted to the study of the adsorption of MgP on the NaCl/Au heterosurface which will also be helpful to directly compare the decoupling performances of NaCl layers and the two types of two-dimensional materials. Heterosurfaces consisting one to three monolayers of NaCl and a Au(111) substrate were constructed to study the NaCl thickness dependent adsorption properties of the MgP molecule by using density functional theory (DFT) calculations. The adsorption energy, charge transfer property and electronic structure of the adsorbed MgP molecule were analyzed.

II. MODEL AND COMPUTATIONAL DETAILS

Top and side views of the heterosurfaces as well as the geometrical configuration of the MgP molecule can be found in FIG. 1. Before constructing the heterosurfaces, we firstly optimized the Au and NaCl in the buck phase to obtain the corresponding lattice constants. The calculated results of 4.10 Å and 5.53 Å for respectively Au and NaCl are in very good agreement with the measured data of 4.08 Å [37] and 5.65 Å [38]. The heterosurfaces were then constructed by adding one to three monolayers of NaCl(100) to a two-layer Au(111) substrate, as shown in FIG. 1 (c). In order to reduce the lattice mismatch, we redefined the Au(111) lattice with a $\begin{pmatrix} 2 & 1 \\ 0 & 1 \end{pmatrix}$ matrix, which gives a $\sqrt{3}\times 1$ cell with lattice constants of a=5.02 Å and b=2.90 Å. The heterosurfaces were then created by using a 4×7 Au(111) slab and 5×5 NaCl(100) supercell. The lattice mismatch of the resulting heterosurfaces was found to be 2.6% and 3.7% in the x and y-directions, respectively. FIG. 1 (a) is the top view of the obtained heterosurface, which has a length of 19.8176 Å (19.9216 Å) in the x (y) direction. To mimic the bulk substrate, the bottom layer of Au(111) was fixed in the simulations. As shown in FIG. 1(a), four representative adsorption sites as defined by the position of the Mg atom in the molecule, namely, the Cl top site (Cl-top), the Na top site (Na-top), the Na–Cl bridge site (b), and the hollow site (h), were selected to study the adsorption of the MgP molecule on the heterosurfaces. To locate the equilibrium adsorption configurations, single-point potential energy scans with respect to the height and rotation energy of the MgP molecule on the heterosurfaces were first performed. Geometrical relaxations were then carried

DOI: 10.1063/1674-0068/cjcp2502015

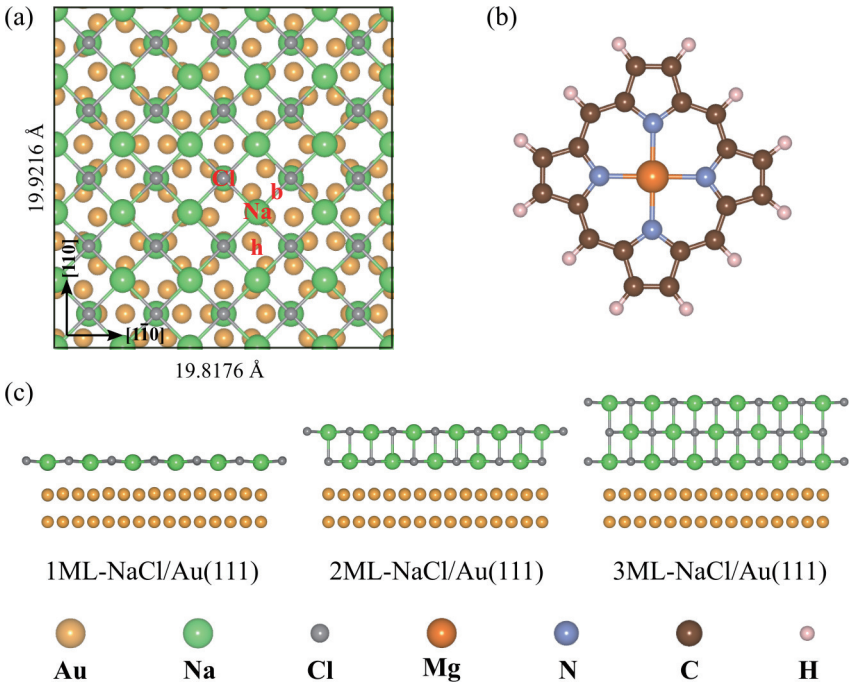

FIG. 1 (a) Top view of the NaCl/Au(111) heterosurface with the four considered adsorption sites (Cl-top, Na-top, bridge, and hollow) as marked by the red letters. (b) Geometrical configuration of the MgP molecule. (c) Side views of the optimized 1ML-NaCl/Au(111), 2ML-NaCl/Au(111), and 3ML-NaCl/Au(111) surfaces.

out for the adsorption site with the lowest energies for each of the three heterosurfaces at the height and rotation angle determined by the energy scan step.

DFT calculations were performed by using the Vienna Ab-initio Simulation Package (VASP) [39]. The Perdew-Burke-Ernzerhof (PBE) functional [40] together with the projector augmented wave (PAW) pseudopotential [41, 42], were applied in all DFT calculations. $1\times1\times1$ and $2\times2\times1$ Monkhorst-Pack grids, together with a 0.02 eV Gaussian broadening, were used for the geometrical optimizations and the single point energy calculations, respectively. The convergence criteria for the electronic and nuclear relaxations were set respectively to 10^{-5} eV and 0.015 eV/Å (except the fixed Au atoms) in the DFT calculations where an energy cutoff of 450 eV was applied. To model the surface, a 15 Å vacuum slab was included for all considered systems. To better describe the van der Waals interactions between the molecule and the surfaces, the DFT-D3(BJ) correction [43] was also considered in the DFT calculations. Precious works have found that the DFT-D3(BJ) correction is sufficient for the description of the adsorption of molecules on the considered surfaces [29, 36]. The Bader charge [44, 45] was used to analyze the charge transfer between the molecule and the surfaces with the help of the VASPKIT program [46]. The VESTA software [47] was applied for the visualization of the DFT results.

III. RESULTS AND DISCUSSION

A. Geometrical configurations of MgP on NaCl/Au(111) surfaces

As mentioned in the previous section, we first scanned the potential energy of the combined systems by changing the height of the MgP molecule on top of the surfaces at each of the four adsorption sites for the three heterosurfaces. For this set of calculations, the molecule was placed on the surfaces by aligning the Mg–N bond with the [1$\bar{1}$0] line of the NaCl surface as shown in FIG. S1 of Supplementary materials (SM). The obtained height dependent potential energy curves are shown in FIG. 2 (a) to (c). From the calculated potential energies, it was found that the Cl-top site has the lowest energy for all three heterosurfaces. The Na-top site leads to the highest energies due to the repulsion between the Mg and Na atoms. It can also be found that the MgP molecule tends to become more distanced (from 3.2 Å to 3.4 Å for the Cl-top configuration) from the surfaces when increasing the thickness of NaCl, which suggests a decrease in the interaction between the surface and the adsorbed molecule.

DOI: 10.1063/1674-0068/cjcp2502015

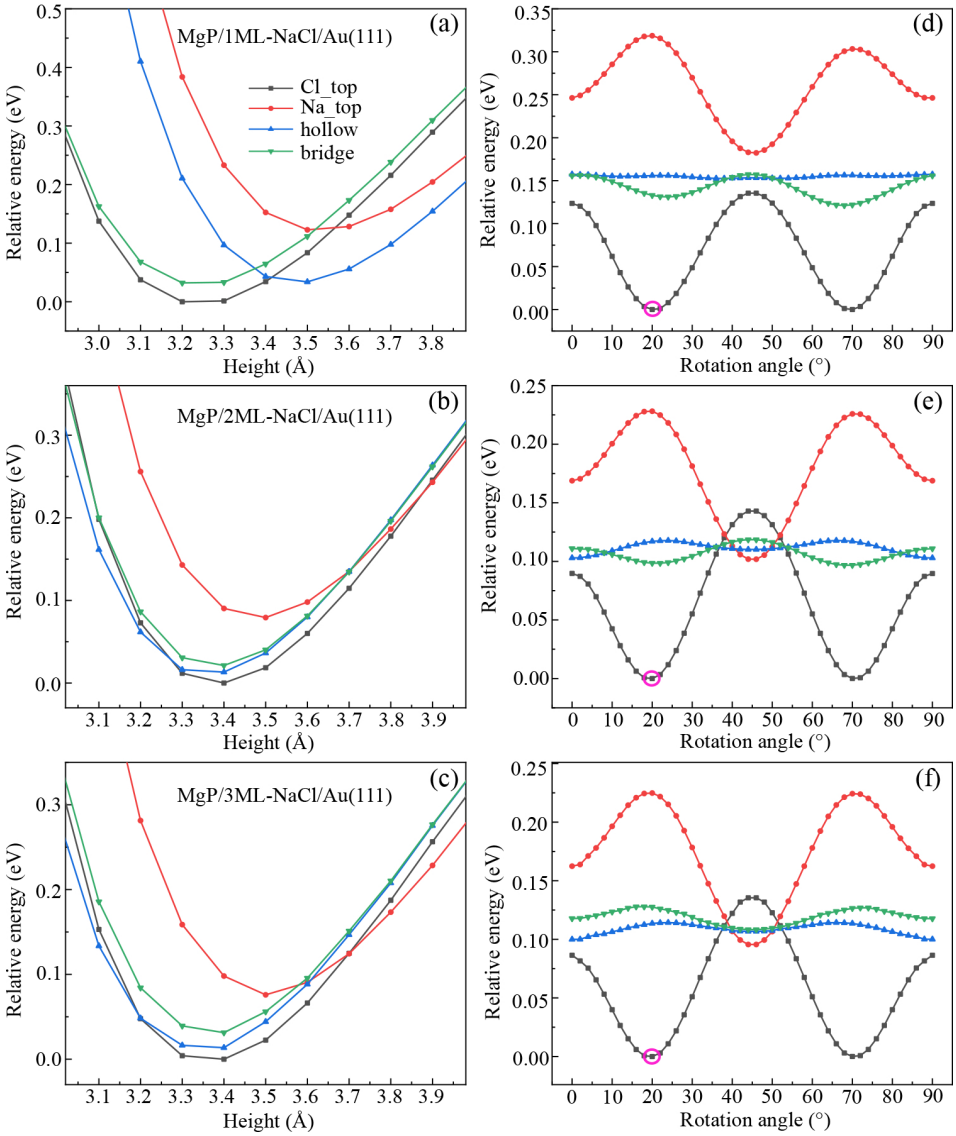

FIG. 2 (a–c) The potential energies as a function of the distance between the MgP molecule and the NaCl/Au(111) surfaces. (d–f) The potential energies as a function of the rotation angle of the MgP molecule as obtained at the height with the lowest energy for each adsorption site. For better comparisons, the energies were shifted by setting the adsorption energy of the Cl-top configuration with the lowest energy to 0 in each of the six cases.

We then scanned the rotation angle-dependent adsorption energies of the molecule on the three types of heterosurfaces at the heights with the lowest energy for each adsorption sites as obtained in FIG. 2 (a) to (c). The MgP molecule has a D_{4h} symmetry, thus, a 90° scan is sufficient for this purpose. The calculation results for the three heterosurfaces can be found in FIG. 2 (d) to (f). The calculated potential energies clear show that a rotation angle of 20° at the Cl-top site gives the lowest adsorption energy for all three cases, as indicated by the pink circles. This result is consistent with previous calculations of the MgP molecule on bare NaCl surface [48]. These three configurations were then fully relaxed to obtain the stable geometries of the considered adsorption systems.

The side and top views of the obtained stable structures of the MgP molecule on the NaCl/Au(111) heterosurfaces together with that on the bare Au(111) surface are shown in FIG. 3. It can be seen that, for all four cases, the Mg atom was "pulled" towards the surfaces, causing the molecule to take a concave configuration instead of the planar structure in the free space. Such nonplanar configurations have indeed been reported before for metalloporphyrins adsorbed on metal surfaces, such as Zn(II) Etioporphyrin I molecule adsorbed on a NiAl(110) [49]. Interestingly, the out-of-plane displace-

DOI: 10.1063/1674-0068/cjcp2502015

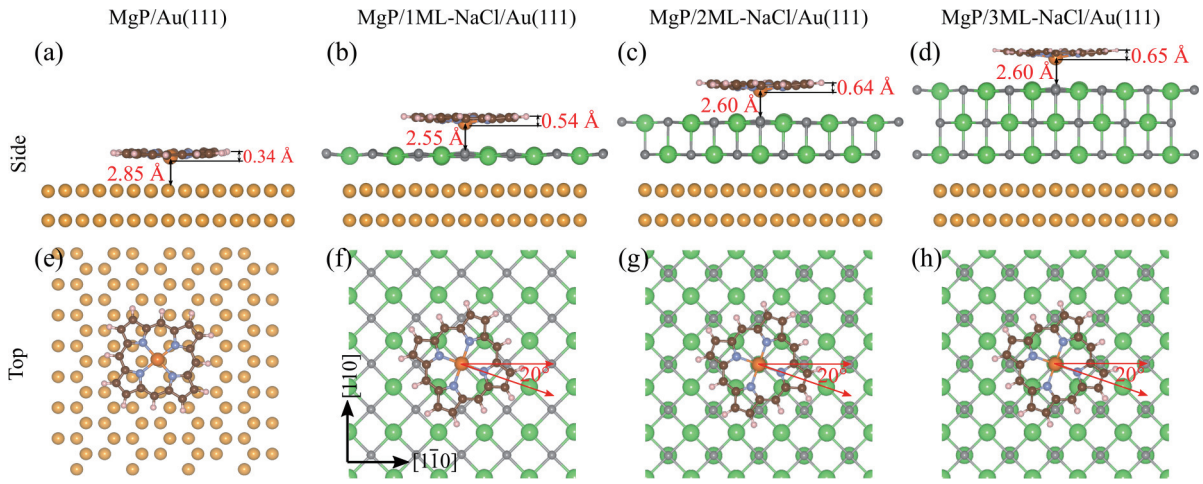

FIG. 3 Side (a–d) and top (e–h) views of the optimized configurations of the MgP molecule on bare Au(111) surface and the three NaCl/Au(111) heterosurfaces.

ment of the Mg atom actually increased when NaCl was included. This should be attributed to the stronger attraction between the charge negative Cl atom and the Mg atom at the more stable Cl-top sites. It can also be found that the distance between the surface and the molecular plane actually decreased from 3.19 Å to 3.09 Å when a single layer of NaCl was included. The distance was then increased to 3.24 Å and 3.25 Å for the surfaces with two and three monolayers of NaCl. The similar distances for the latter two cases suggest that these NaCl layers should be sufficient to screen the influence of the Au substrate on the geometrical structures of the MgP molecule. Interestingly, our previous calculations showed a smaller shift of the Mg atom towards the surface when hexagonal boron nitride and graphene monolayers were applied as the decoupling layers [36]. For all three heterosurfaces, the orientation of the MgP molecule remained to be rotated by 20° with respect to the [1$\bar{1}$0] direction of the NaCl surface. Detailed analysis (as shown in FIG. S2 of SM) on the geometries of the MgP molecule on the four types of surfaces suggests that the bond lengths only underwent rather small changes.

B. Adsorption energy and charge transfer properties

After the adsorption configurations were determined, we then studied the adsorption energies and charge transfer properties of MgP on the four types of surfaces. Such analysis is helpful to understand the influence of the NaCl layers on the interaction between MgP and the metal substrate. The adsorption energy of the molecule is defined as $E_{\rm ads} = E_{\rm tot} - (E_{\rm mol} + E_{\rm sur})$ with $E_{\rm tot}$, $E_{\rm mol}$, and $E_{\rm sur}$ being the total energies of the entire MgP/surface system, the MgP molecule, and the surface, respectively. The calculated adsorption energy and the charge transfer between the MgP molecule and the surfaces are listed in Table I.

TABLE I The adsorption energy and amount of charge that was transferred between the MgP molecule and the heterosurfaces.

Surface	$E_{\rm ads}$/eV	Charge transfer/e$^-$
Au(111)	−3.14	0.40
1ML-NaCl/Au(111)	−1.97	0.20
2ML-NaCl/Au(111)	−1.78	0.03
3ML-NaCl/Au(111)	−1.76	0.03

As shown in Table I, after a single NaCl decoupling layer was added on top of the Au(111) surface, the adsorption energy already increased from −3.14 eV to −1.97 eV. Such a large change in the adsorption energy indicates that the interaction between the MgP molecule and the metal surface was already significantly suppressed by the NaCl monolayer. Increasing the thickness of the NaCl to two monolayers can further reduce the adsorption energy by about 0.2 eV. The adsorption energy then became converged for the cases with two and three monolayers of NaCl, indicating that the interaction between the molecules and the metal surface has been fully isolated, as was found from the geometrical parameters. Our previous work has shown that the adsorption energy of MgP on graphene and hexagonal boron nitride monolayer covered Au(111) surfaces are −1.80 eV and −1.67 eV, respectively [36]. This suggests that such two-dimensional materials and the NaCl multilayers considered in the present work have a similar effect on reducing the molecule–metal interactions.

DOI: 10.1063/1674-0068/cjcp2502015

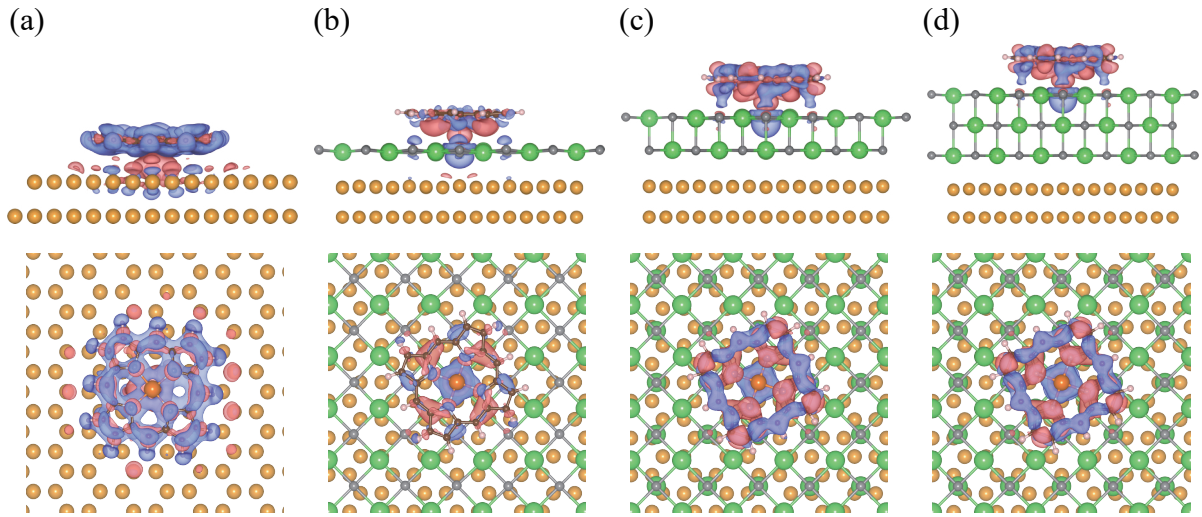

FIG. 4 Side (upper panel) and top (lower panel) views of the differential charge densities for MgP on (a) Au(111), (b) 1ML-NaCl/Au(111), (c) 2ML-NaCl/Au(111), and (d) 3ML-NaCl/Au(111) surfaces. A 5×10^{-4} isovalue was used for the four systems.

A similar trend is also evident from the calculated charge transfer properties based on the Bader charges as can be found in Table I. The calculation result shows that the total charge transferred between the MgP molecule and the bare Au(111) surface is 0.40 e^-. By adding one monolayer of NaCl, the charge transfer is reduced by 50%. After two or three monolayers of NaCl were included, the amount of charge that was transferred to MgP is reduced to 0.03 e^-, indicating almost complete suppression of the charge transfer. In order to better understand the charge transfer properties, we also calculated the differential charge densities ($\Delta\rho$) of the four systems. In practice, $\Delta\rho$ was computed by subtracting the charge densities of the molecule (ρ_m) and the surface (ρ_s) from that of the entire system (ρ_t) as $\Delta\rho = \rho_t - (\rho_m + \rho_s)$. The obtained differential charge densities for the four systems can be found in FIG. 4. Here we used different color to represent the depletion (red) and gain (blue) of electrons.

As shown in FIG. 4(a), it appears that the electron density was attracted by the MgP molecule from the Au atoms below the Mg atom and distributed rather delocalized on the porphyrin ring, causing the MgP molecule to be partially negatively charged. After one monolayer of NaCl was included, as shown in FIG. 4 (b), the charge transfer becomes more confined to the area between the NaCl and the MgP plane. Although the Mg atom still attracts electron from the surface, the NaCl layer also starts to gain electrons from the molecule, thus reducing the overall charge transfer. It can also be found that the Au(111) surface still has noticeable contributions to the charge transfer process. For the cases with two or three monolayers of NaCl, as depicted in FIG. 4 (c) and (d), the charge transfer distribution remained approximately the same, and there was no direct charge transfer from Au(111) to the MgP molecule. Compared to that with only a single monolayer of NaCl, the molecular charge density appears to become larger with the increase of the layers of NaCl although the overall charge transfer was further reduced as shown in Table I. The increased charge density distribution could be attributed to two primary factors. Firstly, multilayer of NaCl facilitates the formation of a vertical dipole moment through Mg-Cl-Na, which appears to have more profound influence on the charge transfer than the Mg-Cl-Au arrangement observed in one monolayer of NaCl. Secondly, the non-planar positioning of Mg atoms relative to the molecular plane can also induce charge density redistribution along the C–C skeleton through Mg–N bonding interactions. This is in line with the changes to the adsorption configurations where the out-of-plane displacement of Mg becomes more pronounced in systems with two and three NaCl layers, as quantified in FIG. 3. However, unlike the single monolayer case where it is rather localized between the MgP and the NaCl layer, the differential charge density becomes more evenly distributed on the molecule in the z-direction. As a result, the depletion and gain of electrons by the molecule also becomes rather balanced and resulted in the almost completely

DOI: 10.1063/1674-0068/cjcp2502015

suppressed charge transfer between the surfaces and the MgP molecule.

C. Partial density of states of the MgP molecule

To gain more insight into the influence of the NaCl layers on the electronic structure of the MgP molecule, we also analyzed the partial density of states (PDOS) of the four systems in FIG. 5. In order to demonstrate the hybridization of the molecular electronic structure with the surfaces, the PDOS of the MgP molecule in vacuum was also included in FIG. 5 as blue dashed lines.

For the case where the molecule is directly adsorbed on the Au(111) surface, as shown in FIG. 5(a), the PDOS of the MgP molecule is clearly broadened and shifted when compared to those obtained in the free space. This demonstrates the rather strong influence of the Au substrate on the electronic structure of the MgP molecule, which causes the molecular orbitals to hybridize with the electronic structure of Au. After a single monolayer of NaCl is added on the gold surface, the PDOS of the MgP molecule started to show more molecular-like characteristics with narrow and discrete peaks. Especially, the frontier molecular orbitals around the Fermi energy already resemble nicely those of the free MgP molecule. There is still some hybridization between the molecule and the surface, which causes the peaks in the PDOS to be slightly broadened with reduced height. Such hybridization between the molecule and the surface is further suppressed when two monolayers of NaCl are inserted between the MgP molecule and the Au(111) surface. As can be found in FIG. 5(c), all the characteristic peaks of the PDOS in the energy range of −2.0 eV to 4.0 eV have a similar shape to those of the free molecule. This suggests that the molecular electronic structure near the Fermi energy can already be nicely preserved when two monolayers of NaCl are applied as the decoupling layer. The case with three monolayers of NaCl is similar to that obtained with two monolayers, as shown in FIG. 5(d). In this case, the PDOS around the Fermi energy is almost the same as that obtained in the free space, indicating that the molecule is completely isolated from the Au(111) surface. It should be mentioned that the Mg atom does not contribute significantly to the frontier MOs of the MgP molecule, as can be found from the calculated element specific projected density of states in FIG. S3 (SM). This is the main reason that the spatial change of the Mg atom (as shown in FIG. 3) barely affects the electronic structure of the frontier MOs. These results suggests that two or more monolayers of NaCl are sufficient to decouple the molecule from the metallic substrate.

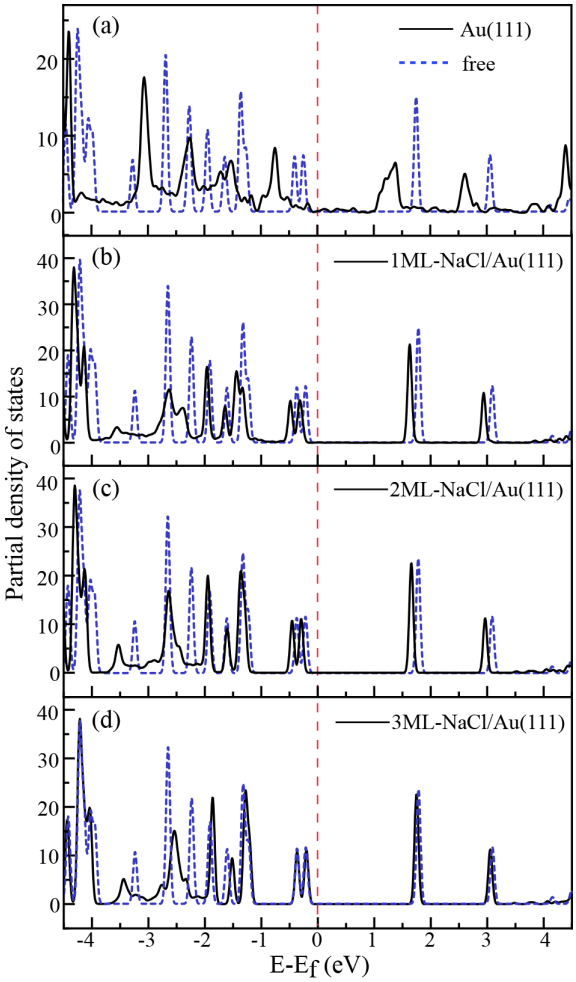

FIG. 5 PDOS of the MgP molecules as adsorbed on (a) Au(111), (b) 1ML-NaCl/Au(111), (c) 2ML-NaCl/Au(111), and (d) 3ML-NaCl/Au(111) surfaces. The blue dashed line represents the PDOS of the free MgP molecules. Here the Fermi energy was set to 0, as marked by the vertical red line.

It is worth to mention that stronger hybridization of electronic structures between MgP and the substrate can be found at about 2.0 eV below the Fermi energy. Such hybridization should be attributed to the interaction between MgP and NaCl, since the Au substrate has already been fully decoupled. This is also supported by the calculated PDOS of the NaCl layers (FIG. S4 in SM) which clearly shows that the PDOS of the NaCl layers are mainly located in the occupied region at about 2 eV below the Fermi energy.

IV. CONCLUSION

In this work, we studied the adsorption of a MgP molecule on bare Au(111) and NaCl-covered Au(111)

DOI: 10.1063/1674-0068/cjcp2502015

surfaces by using DFT calculations. The stable adsorption configurations and electronic structures of the MgP molecule on Au(111), 1ML-NaCl/Au(111), 2ML-NaCl/Au(111), and 3ML-NaCl/Au(111) surfaces were obtained. The Cl-top site, with a rotation angle of 20° between the Mg–N bond of the MgP molecule and the [1$\bar{1}$0] direction of the NaCl surface, was found to be the most stable adsorption site. Calculated adsorption energies and charge transfer properties show that a single monolayer of NaCl can already significantly reduce the molecule–metal interaction. After two or three monolayers of NaCl were added on top of the Au(111) surface, the charge transfer between the MgP molecule and the surfaces was almost completely suppressed. By comparing the PDOS of the adsorbed MgP to those obtained in vacuum, it was found that the NaCl layers can significantly reduce the metal surface caused hybridization of the molecular electronic structure. Especially, the PDOS obtained with two and three layers of NaCl were almost the same as that of the free molecule near the Fermi energy, demonstrating that the electronic structure of the molecule is well preserved in such cases. These results indicate that the MgP molecule can be considered as being electronically decoupled from the Au(111) surface after two or more NaCl monolayers are added to the substrate.

Supplementary materials: Initial configuration of the system for the potential energy scan, detailed analysis on the molecular bond lengths before and after adsorption, projected density of states of the MgP molecule, PDOS of the three NaCl layers, charge transfer between Au and NaCl, and work functions of the surfaces are available. Cartesian coordinates of the optimized geometries at the most stable adsorption sites.

V. ACKNOWLEDGMENTS

This work was supported by the National Natural Science Foundation of China (No.22373084, No.62201494), Hebei Natural Science Foundation (B2022203007), and the Cultivation Project for Basic Research and Innovation of Yanshan University (2024LGZD002).

[1] Z. Ma and F. Zaera, Surf. Sci. Rep. **61**, 229 (2006).
[2] T. Bligaard, J. Nrskov, S. Dahl, J. Matthiesen, C. Christensen, and J. Sehested, J. Catal. **224**, 206 (2004).
[3] C. Joachim and M. A. Ratner, Proc. Natl. Acad. Sci. USA **102**, 8801 (2005).
[4] J. Repp, G. Meyer, S. M. Stojkovixc, A. Gourdon, and C. Joachim, Phys. Rev. Lett. **94**, 026803 (2005).
[5] L. Gross, N. Moll, F. Mohn, A. Curioni, G. Meyer, F. Hanke, and M. Persson, Phys. Rev. Lett. **107**, 086101 (2011).
[6] S. Schintke, S. Messerli, M. Pivetta, F. Patthey, L. Libioulle, M. Stengel, A. De Vita, and W. D. Schneider, Phys. Rev. Lett. **87**, 276801 (2001).
[7] N. Nilius, T. M. Wallis, and W. Ho, Phys. Rev. Lett. **90**, 046808 (2003).
[8] J. Libuda, F. Winkelmann, M. Bäumer, H. J. Freund, T. Bertrams, H. Neddermeyer, and K. Müller, Surf. Sci. **318**, 61 (1994).
[9] X. H. Qiu, G. V. Nazin, and W. Ho, Science **299**, 542 (2003).
[10] A. J. Heinrich, J. A. Gupta, C. P. Lutz, and D. M. Eigler, Science **306**, 466 (2004).
[11] N. Nilius, N. Ernst, and H. J. Freund, Phys. Rev. Lett. **84**, 3994 (2000).
[12] X. Lin, J. C. Lu, Y. Shao, Y. Y. Zhang, X. Wu, J. B. Pan, L. Gao, S. Y. Zhu, K. Qian, Y. F. Zhang, D. L. Bao, L. F. Li, Y. Q. Wang, Z. L. Liu, J. T. Sun, T. Lei, C. Liu, J. O. Wang, K. Ibrahim, D. Leonard, W. Zhou, H. M. Guo, Y. L. Wang, S. X. Du, S. T. Pantelides, and H. J. Gao, Nat. Mater. **16**, 717 (2017).
[13] N. Krane, C. Lotze, G. Reecht, L. Zhang, A. L. Briseno, and K. J. Franke, ACS Nano **12**, 11698 (2018).
[14] G. Reecht, N. Krane, C. Lotze, and K. J. Franke, ACS Nano **13**, 7031 (2019).
[15] G. Reecht, N. Krane, C. Lotze, L. Zhang, A. L. Briseno, and K. J. Franke, Phys. Rev. Lett. **124**, 116804 (2020).
[16] M. Jana, R. Xu, X. B. Cheng, J. S. Yeon, J. M. Park, J. Q. Huang, Q. Zhang, and H. S. Park, Energy Environ. Sci. **13**, 1049 (2020).
[17] K. Miwa, H. Imada, S. Kawahara, and Y. Kim, Phys. Rev. B **93**, 165419 (2016).
[18] F. F. Kong, X. J. Tian, Y. Zhang, Y. J. Yu, S. H. Jing, Y. Zhang, G. J. Tian, Y. Luo, J. L. Yang, Z. C. Dong, and J. G. Hou, Nat. Commun. **12**, 1280 (2021).
[19] S. Fölsch, A. Helms, S. Zöphel, J. Repp, G. Meyer, and K. H. Rieder, Phys. Rev. Lett. **84**, 123 (2000).
[20] X. Sun, M. P. Felicissimo, P. Rudolf, and F. Silly, Nanotechnology **19**, 495307 (2008).
[21] Y. Zhang, Y. Luo, Y. Zhang, Y. J. Yu, Y.M. Kuang, L. Zhang, Q. S. Meng, Y. Luo, J. L. Yang, Z. C. Dong, and J. G. Hou, Nature **531**, 623 (2016).
[22] B. Doppagne, M. C. Chong, H. Bulou, A. Boeglin, F. Scheurer, and G. Schull, Science **361**, 251 (2018).
[23] K. Kimura, K. Miwa, H. Imada, M. Imai-Imada, S.

DOI: 10.1063/1674-0068/cjcp2502015

Kawahara, J. Takeya, M. Kawai, M. Galperin, and Y. Kim, Nature **570**, 210 (2019).
[24] Y. Luo, G. Chen, Y. Zhang, L. Zhang, Y. Yu, F. Kong, X. Tian, Y. Zhang, C. Shan, Y. Luo, J. Yang, V. Sandoghdar, Z. Dong, and J. G. Hou, Phys. Rev. Lett. **122**, 233901 (2019).
[25] J. Doležal, S. Canola, P. Hapala, R. C. de Campos Ferreira, P. Merino, and M. Švec, Nat. Commun. **13**, 6008 (2022).
[26] B. Yang, G. Chen, A. Ghafoor, Y. Zhang, Y. Zhang, Y. Zhang, Y. Luo, J. Yang, V. Sandoghdar, J. Aizpurua, Z. Dong, and J. G. Hou, Nat. Photon. **14**, 693 (2020).
[27] H. Imada, M. Imai-Imada, K. Miwa, H. Yamane, T. Iwasa, Y. Tanaka, N. Toriumi, K. Kimura, N. Yokoshi, A. Muranaka, M. Uchiyama, T. Taketsugu, Y. K. Kato, H. Ishihara, and Y. Kim, Science **373**, 95 (2021).
[28] K. Kaiser, L. A. Lieske, J. Repp, and L. Gross, Nat. Commun. **14**, 4988 (2023).
[29] J. Xiao, W. Zhao, L. Li, L. Ma, and G. Tian, Phys. Chem. Chem. Phys. **25**, 6060 (2023).
[30] G. Tian, F. Qiu, C. Song, S. Duan, and Y. Luo, J. Phys. Chem. Lett. **12**, 9094 (2021).
[31] J. Otsuki, Coord. Chem. Rev. **254**, 2311 (2010).
[32] W. Auwärter, D. Ecija, F. Klappenberger, and J. V. Barth, Nat. Chem. **7**, 105 (2015).
[33] J. M. Gottfried, Surf. Sci. Rep. **70**, 259 (2015).
[34] S. W. Wu, G. V. Nazin, and W. Ho, Phys. Rev. B **77**, 205430 (2008).
[35] C. Chen, P. Chu, C. A. Bobisch, D. L. Mills, and W. Ho, Phys. Rev. Lett. **105**, 217402 (2010).
[36] W. Zhao, J. Xiao, Z. Ma, L. Ma, and G. Tian, Phys. Rev. B **110**, 205410 (2024).
[37] B. N. Dutta and B. Dayal, Phys Status Solidi B **3**, 473 (1963).
[38] S. Froyen and M. L. Cohen, Phys. Rev. B **29**, 3770 (1984).
[39] G. Kresse and J. Furthmüller, Phys. Rev. B **54**, 11169 (1996).
[40] J. P. Perdew, K. Burke, and M. Ernzerhof, Phys. Rev. Lett. **77**, 3865 (1996).
[41] P. E. Blöchl, Phys. Rev. B **50**, 17953 (1994).
[42] G. Kresse and D. Joubert, Phys. Rev. B **59**, 1758 (1999).
[43] S. Grimme, S. Ehrlich, and L. Goerigk, J. Comput. Chem. **32**, 1456 (2011).
[44] G. Henkelman, A. Arnaldsson, and H. Jxonsson, Comp. Mater. Sci. **36**, 354 (2006).
[45] W. Tang, E. Sanville, and G. Henkelman, J. Phys.: Condens. Matter. **21**, 084204 (2009).
[46] V. Wang, N. Xu, J. C. Liu, G. Tang, and W. T. Geng, Comput. Phys. Commun. **267**, 108033 (2021).
[47] K. Momma and F. Izumi, J. Appl. Crystallogr. **44**, 1272 (2011).
[48] S. Yan, Z. Ding, N. Xie, H. Gong, Q. Sun, Y. Guo, X. Shan, S. Meng, and X. Lu, ACS Nano **6**, 4132 (2012).
[49] X. H. Qiu, G. V. Nazin, and W. Ho, Phys. Rev. Lett. **93**, 196806 (2004).

DOI: 10.1063/1674-0068/cjcp2502015